Possibilities for High-Energy Chopper Spectrometers at the SNS

Written for the ARCS Instrument Development Team meeting 4/30/01 in Pasadena, CA

Doug Abernathy
4/23/01

This brief report lays out six possible chopper spectrometer configurations, taking into account the physical constraints of the SNS target building as currently known. The performance of these instruments are compared in terms of the flux of neutrons on the sample for a given elastic energy resolution, as well as other figures of merit.

Background

The current target building and instrument configuration is shown in Figure 1. Of course, most of these instruments are placeholders, but the high-resolution backscattering spectrometer (beamline 2) and the magnetism and liquids reflectometers (4A and 4B) are in the SNS baseline and are proceeding with engineering design. Several more instruments are approved by the Experimental Facilities Advisory Committee and/or have claimed spots around the target: SANS (6), engineering (9), powder (11A), disordered materials (10) and the multichopper spectrometer CNCS (5). The layout of the target building itself is almost fixed as well, since the pilings to hold the building are now in place at Oak Ridge and the concrete work forming the hard constraints for the instrument floor will be contracted out soon.

High-energy chopper spectrometers have always been considered essential for the SNS. A number of working groups and committees advising the SNS have spelled out desired characteristics. Typically these have fallen into two general instrument categories – a high-intensity spectrometer with large angular coverage and a high-resolution spectrometer. How one could place both such instruments on the SNS target was the subject of a report to the SNS Instrument Oversight Committee (now EFAC) in June 2000 [Ref. 1]. The layout is shown in Fig. 1 on beamlines 17 and 18, with a smaller but large coverage instrument tucked next to the proton transport line and a higher resolution instrument using some space behind the smaller one. The recommendation for the committee was that the two-spectrometer concept was sound, with a preference given for developing the high-resolution spectrometer first.

Given the opportunity of an outside Instrument Development Team building a high-energy chopper spectrometer with DOE funding not coming directly from the SNS budget, it makes sense to reevaluate the current concepts for SNS chopper spectrometers. The IDT may decide new priorities, and avoid some compromises that instruments within the SNS have been asked to accept in order to have more instruments funded. This report attempts to describe the constraints and optimization principles that should be respected, and gives six example instrument configurations for evaluation by the IDT. It is hoped that one or two concepts will emerge that will lead quickly to the submission of a proposal for funding with the DOE.

General optimization and constraints

There are many attributes for the design of a spectrometer that should be considered in determining the most appropriate concept for a given scientific program, including the flux of neutrons on the sample for a desired energy resolution, detector coverage, Q-resolution, need for single crystal capabilities or polarization analysis, ease of use and sample change-out, special sample environments, cost, etc. For the purposes of this evaluation the primary focus will be on maximizing the flux for a given resolution and sample-detector distance, and combining those considerations with the detector coverage. Questions concerning the Q-resolution and possible enhancements from using neutron guides will be left for another discussion.

The first choice for an instrument is to determine which moderator it would use. For a high-energy direct-geometry chopper the ambient water moderator (bottom upstream) at the SNS is best, both because its position along the target optimizes the flux from the moderator and the thermal neutron spectrum is enhanced compared to the other cold SNS moderators. The performance of this moderator has been calculated by Monte Carlo simulation and used in an approximate analytic formula to determining the instrument flux and resolution, as described in the appendix in reference 1.

Several general optimizing principles emerge in considering the flux onto the sample for a given desired energy resolution:

1. The secondary flightpath L_3 (sample-detector) should be as long as possible. The only constraints on L_3 are practical ones, such as space limitations to achieving a desired angular coverage or the cost of large detector areas.
2. The Fermi chopper-sample distance L_2 should be as small as possible. The constraint is that for the lowest scattering angles the Fermi chopper may scatter direct beam into the detectors. Sufficient space between the chopper and sample will eliminate this source of background. For the present discussion we take this distance to be 2m.
3. Given L_2, L_3 and energy resolution, there will be an optimum moderator-chopper distance L_1. At too small a distance the moderator width will not allow the desired energy resolution to be achieved, while at too large a distance the fall off of solid angle from the source causes the flux to fall. As shall be seen, for the SNS it is very difficult to optimize L_1 for energy resolutions above about 2 or 3%, due to the massive target monolith shielding and the closeness of adjacent beamlines.

These principles must be combined with the target building constraints.

The desired location for a chopper spectrometer is a beamline with maximum room near the target viewing the water moderator (beamlines 7-9 and 16-18). After discussions with the target group and architects, beamline 9 does not afford a very flexible or useful space for a close-in instrument. The target handling facility must use space near the target for manipulators, and below the beamline there are rooms in the basement precluding any pit in the floor. It was therefore decided to concentrate on the area around beamlines 17 and 18 for placement of the instrument.

Figure 2 shows this area and some of the constraints it imposes, taken from the current architects drawings of the target building. The ring-target beam transport (RTBT) tunnel forms one wall of the beamline 18 area. Also at beamline 18 is a building column, which despite long discussions cannot be eliminated from the experimental area. There is an instrument pit, roughly 2m deep, covering the areas of beamline 17 and 18 in anticipation of large detector arrays. One constraint not shown is an overhang from the proton transport line, which extends out to the position of the building column at beamline 18.

Besides the building constraints, the adjacent beamlines limit the area available for placing instruments as well. Because of the high power of the SNS, it has been calculated that each line needs roughly 2m of shielding in any direction to meet the goal of 0.25 mrem/hr in the target hall. Thus the shielding for each line overlaps with its neighbor out to roughly 17m, and subsequently starts to diminish in size because of the fall off in intensity moving away from the source. Within 17m the bisector between two lines is taken as the limit for installing equipment. One problem this fails to address is whether the instrumental background will be low enough if the detectors are mounted close to an adjacent beamline. This will have to be evaluated as well as possible with modeling of the neutron and gamma "leakage" from the shielding. A similar concern applies to the proton-transport tunnel, which encloses beam collimation for the protons going to the target.

Instrument Models

Given the above optimization goals and constraints, six models for chopper spectrometers have been made in an attempt to explore the possible configuration space and shed some light on the best compromises for the science to be done. The models have not been taken to much detail, but have been roughly laid out to conform to the existing building constraints. It has been assumed that a minimum of 30cm additional shielding of borated wax cans or other material will be needed around the detectors, in addition to space for mounting. For short secondary flightpaths, an additional 30cm is allowed, with the assumption that access will be from above or below. Larger flightpaths have additional space since it may not be possible to get below to service detectors. For configurations that go to large scattering angle, a consistent maximum of 140˚ has been adopted. Where possible, the detectors cover ±30˚ in the plane parallel to the direction the sample is inserted.

The basic parameters for the different models are given in Table 1. Plan views and a 3-dimensional drawings are attached at the end of the report. Comments about the different models, the defining constraints and the advantages and disadvantages are:

Model A: Small, horizontal geometry on 18 with full angular coverage at a single flightpath. The secondary flightpath was maximized subject to the constraints of the building column and the tunnel wall. This corresponds to a configuration examined in reference 1. *Pros*: Single flightpath length out to large angles for simpler data comparison and subtraction, very large angular coverage. *Cons*: Smaller flux at a given resolution than larger flightpath instrument, Q-resolution worse given same detector size as larger flightpath instrument.

Model B: Small, vertical geometry on 18 with large angular coverage at a single flightpath. In order to get closer to the moderator, the angular coverage in the horizontal was reduced to avoid intruding into the adjacent beamline shielding. *Pros*: Single flightpath, fairly large solid angle coverage, closest to moderator. *Cons*: Detectors may be subject to background from adjacent beamline, lower flux and worse Q-resolution than larger flightpath instrument. Horizontal sample access may make some sample environments difficult.

Model C: Large, vertical geometry on 18 with large angular coverage at a single flightpath. The sample was positioned to allow a 5m secondary flightpath to large angles, constrained by the adjacent beamline and the proton tunnel overhang. *Pros*: Large flightpath out to high angles at a moderate distance from the source. *Cons*: Restricted horizontal angular coverage due to adjacent beamline. Horizontally mounted sample environment.

Model D: Two flightpath, horizontal geometry on 18. Position determined as in Model A, with transition to a larger flightpath at an angle determined by the building column. *Pros*: Combines closer instrument with larger flightpath for some part of the coverage. *Cons*: Two flightpaths may confuse data analysis, advantage of larger flightpath may not extend to high enough angles.

Model E: Two flightpath, horizontal geometry on 17. Position determined by achieving -30˚ scattering angle in low-angle bank subject to constraint of beamline 16B shielding. *Pros*: Has more angular coverage at large secondary flightpath. *Cons*: May not be acceptable because of crowding of beamline 18, two flightpaths may confuse data analysis.

Model F: Single, large flightpath with smaller angular coverage on 17. Position determined as for Model E. *Pros*: Has good resolution for the low angle bank, could co-exist with Model A or other small instrument on beamline 18. *Cons*: Sacrifices higher angles to avoid neighbors, may still have problems with beamstop for a short instrument on beamline 18 and with background from beamline 16B.

Model	Incident flightpath $L_1 + L_2$ (m)	Low-angle bank			High-angle bank		
		L_3 (m)	Horz. (º)	Vert.(º)	L_3 (m)	Horz. (º)	Vert.(º)
A	13.6	3.0	-30,140	±30			
B	12.5	3.0	±20	-45,140			
C	15.0	5.0	±20	-35,60	5.0	±10	60,140
D	13.6	5.5	-20,40	±30	3.0	40,140	±30
E	17.5	5.5	-30,60	±30	3.0	60,140	±30
F	17.5	5.5	-30,60	±30			

Table 1. Basic parameter of chopper spectrometer models.

Performance comparisons

The analytic model for chopper performance derived by Toby Perring and described in the appendix of reference 1 has been used to compare the different chopper models presented above. Figure 3 illustrates the dependence of the flux on the sample for given secondary spectrometer length and elastic energy resolution as the moderator-sample distance is varied. Note that at each position the Fermi chopper slit package spacing is chosen to satisfy the required resolution, if possible. Results for 63meV and 250meV are plotted for L_3 equal to 3.0m and 5.5m. In all cases there is the characteristic quick rise to an optimum value, then a slow fall off. For larger L_3 the optimum position moves inward, since the better resolving power in the secondary spectrometer relaxes the requirements on the incident resolution.

Relaxing the energy resolution moves the optimum moderator-distance to smaller values. These curves show that given the physical constraints of the SNS target, it is not possible to reach an optimum configuration for energy resolutions greater than about 2%. It is not possible to construct a "high-flux" configuration that is optimized at 5%, for example. Of course, by relaxing the Fermi chopper slit package one can still gain in flux at the expense of resolution - a situation that is typical of single crystal experiments at the MAPS spectrometer.

There is a systematic shift of the curves to longer distances for 63meV compared to 250meV. This is due to the relatively deep poison depth chosen for the moderator, which has its greatest effect in the thermal range, and no effect in the epithermal region. The trade-off in flux and pulse width, and therefore chopper performance, will be investigated further. Since the spectrometer energy resolution is already in the 2% range at the peak energy for thermalization, it will probably be best to keep the greater than linear flux gain that comes with the pulse width gain at larger poison depths.

Table 2 shows some of the instrument parameters that can be derived from the basic dimensions listed in Table 1. The solid angle coverage of each bank of detectors is listed for the six models, as well as the total solid angle and total detector area. Also shown in Table 2 is a crude estimate of the basic cost of the instrument configuration, calculated by a simple scalable cost model for chopper spectrometers. In this model some simplistic estimates of how costs will scale with dimensions of the instrument are made. The shaded cells in the example cost sheet shown in Table 3 are calculated from the basic parameters of the instrument model D. There are $5.5 million in costs that do not vary from model to model, and no particular care has been taken to provide contingency.

Model	Low-angle bank solid angle (ster)	High-angle bank solid angle (ster)	Total solid angle (ster)	Total area (m^2)	Cost estimate (M$)
A	3.0	0.0	3.0	26.7	9.4
B	2.2	0.0	2.2	19.9	8.9
C	1.1	0.5	1.6	40.5	12.2
D	1.1	1.7	2.8	47.4	12.5
E	1.6	1.4	3.0	60.1	14.2
F	1.6	0.0	1.6	47.6	12.5

Table 2. Parameter derived for the different chopper spectrometer models.

ITEM	Unit	Unit Cost (k$)	Mat'l Qty.	Cost (k$)
Detectors and Data Acquisition				**4512**
Low-angle LPSDs	ea	2.0	975	1939
High-angle LPSDs	ea	1.9	518	960
LPSD Electronics	ea	1.0	1493	1493
Beamline Controls/DAQ	ea	120.0	1	120
Primary flightpath				**930**
Core vessel insert	ea	50.0	1	50
Shutter insert	ea	50.0	1	50
T0 Horizontal Axis Chopper	ea	150.0	1	150
Disk Chopper	ea	100.0	1	100
E0 Fermi Chopper	ea	150.0	2	300
Variable Aperatures	ea	30.0	4	120
Beamline Roughing Pump	ea	8.0	2	16
Neutron Guide	m	15.5	7.35	114
Guide casing and fixed apertures	m	2.0	7.35	15
Beam Monitors	ea	5.1	3	15
Secondary Spectrometer				**1421**
Sample Vessel	m^2	6.0	6.28	38
Low-angle Vessel	m^2	6.0	128.28	770
High-angle Vessel	m^2	6.0	50.95	306
Goniometer/Thimble	ea	80.0	1	80
Radial Collimator	ea	40.0	1	40
Safety Interlocks	ea	20.0	1	20
Vacuum Roughing Pump	ea	12.0	2	24
Vacuum Cryopump/Turbopump	ea	144.0	1	144
Shielding				**1472**
Incident Beamline/Shielding	m	60.0	6.60	396
Beam Stop	ea	90.0	1	90
Vessel Internal Shielding	m^2	0.5	179.23	90
Vessel Shielding - Wax Cans	m^2	5.0	179.23	896
Sample Environment				**138**
Cryofurnace	ea	27.5	1	28
Displex	ea	34.1	1	34
Furnace	ea	71.7	1	72
Temperature Controller	ea	4.5	1	5
Miscellaneous				**185**
Mezzanine	ea	100	1	100
Control cabin and furniture	ea	40	1	40
Tool Box & Tools	ea	5.0	1	5
Miscellaneous Supports/Hardware	ea	25.0	1	25
Instrument Services	ea	15.0	1	15
MAT'L TOTAL				***8658***
Personnel and Travel				**3820**
Instrument Scientist/Project Manager	FTE	130	4	520
Project Engineer	FTE	175	4	700
Designer	FTE	115	4	460
Caltech project support	0.2FTE	30	4	120
ANL project support	0.2FTE	30	4	120
Installation at ORNL	ea	1000	1	1000
Support for Scientific Software	ea	900	1	900
TOTAL				***12478***

Table 3. Example cost estimate for model D spectrometer.

The dependence of the flux on the sample versus the required elastic energy resolution is plotted in Figure 4 for 63meV and 250meV. Here the models are split into different detector banks which share the same sample-moderator and secondary spectrometer lengths. Again, there is a difference in the form of the curves when the moderator is thermalizing the neutrons and in the epithermal region. The two banks that are close to the target and small cannot achieve better than about 2% elastic energy resolution at 63meV. The large bank located closer to the target provides the best flux in all cases unless the resolution is pushed to the lowest extremes.

Of course, there are any number of other figures-of-merit that would emphasize different aspects of the comparison among the different models. Two choices are plotted in figures 5 and 6. Figure 5 (FoM1) shows the results of plotting the product of the total solid angle coverage of the model and the flux-on-sample found for the lowest resolution bank of the model. This assumes that all solid angle coverage contributes equally to the merit of the instrument, and it underemphasizes the additional information in a detector bank with longer flightpath. It is interesting that in this comparison Model A has a higher figure-of-merit than Model B. This demonstrates the compromise in angular coverage necessary in going to a vertical geometry and moving in towards the target may not be worthwhile.

Figure 6 (FoM2) plots the sum of the solid angle time flux for low- and high-angle detector banks for each model. Each bank is considered separately in calculating the flux for a given resolution, so this figure-of-merit could not be achieved in practice since there is only one choice of Fermi chopper slit package at a time. Nevertheless, this is an attempt to capture the added value of having combined large and small flightpaths on the same instrument. FoM2 is the same as FoM1 for a single secondary flightpath instrument. In this case, Model D is seen to be the most desirable because it combines the benefits of the larger flightpath at a position closer to the moderator.

Conclusions

This report presents six alternative models for chopper spectrometers at the SNS. This is of course not an exhaustive list of possibilities, but is an attempt to show a variety of instruments. Each experiment has its own figure-of-merit, but some simple performance measures are presented to illustrate the trade-offs among the different concepts. In particular, using a vertical scattering geometry does allow on to have a continuous coverage of large secondary flightpath, but at a cost in terms of solid angle coverage and presumably in ease of use of sample environment equipment.

There are many other consideration beyond the performance measured used in this report. Q-resolution may be a factor, as well as a view to how adjacent beamlines will be developed in the future. It is worth considering whether it is better to build a more complete instrument with a smaller scale, or reduce some cost of a larger instrument by leaving off detectors that could be installed in the future.

References

[1] “Conceptual Design and Performance of Two Chopper Spectrometers for the SNS,” D. L. Abernathy, June 6, 2000, SNS document IS-1.1.8.4-6033-RE-A-00.

QTY	CAGE CODE	PART OR IDENTIFYING NO	NOMENCLATURE OR DESCRIPTION	L1	FIND NO	MODERATOR (K)
1		BEAMLINE 18 BU	WIDE ANGLE CHOPPER SPECTROMETER	12.5 m	24	H2O (300 K)
1		BEAMLINE 17 BU	1% CHOPPER SPECTROMETER	17.0 m	23	POISONED
1		BEAMLINE 16 BU	16B PROTOTYPING BEAM	19.0 m	22	DECOUPLED
1		BEAMLINE 16 BU	16A POLARIZED DIFFRACTOMETER	38.0 m	21	
1		BEAMLINE 15 BD	NEUTRON OPTICS DEVELOPMENT	17.0 m	20	SUPER-CRITICAL H2
1		BEAMLINE 14 BD	14A SPIN-ECHO SPECTROMETER	20.0 m	19	NON-POISONED (20 K)
1		BEAMLINE 14 BD	14B SPIN-ECHO SANS	15.0 m	18	COUPLED
1		BEAMLINE 13 BD	FUNDAMENTAL PHYSICS	15.0 m	17	
1		BEAMLINE 12 TU	SINGLE CRYSTAL DIFFRACTOMETER	12.0 m	16	SUPER-CRITICAL H2
1		BEAMLINE 11 TU	11A POWDER DIFFRACTOMETER	60.0 m	15	POISONED (20 K)
1		BEAMLINE 11 TU	11B DIFFUSE/CRITICAL SCATTERING SINGLE CRYSTAL DIFFRACTOMETER	20.0 m	14	DECOUPLED
1		BEAMLINE 10 TU	DISORDERED MATERIALS INSTRUMENT	15.0 m	13	
1		BEAMLINE 09 BU	ENGINEERING DIFFRACTOMETER	44.0 m	12	H2O (300 K)
1		BEAMLINE 08 BU	8B MULTI-INSTRUMENT BEAMLINE	50.0 m	11	POISONED
1		BEAMLINE 08 BU	8A MOLECULAR SPECTROMETER	25.0 m	10	DECOUPLED
1		BEAMLINE 07 BU	HIGH-Q/HIGH INTENSITY SINGLE CRYSTAL DIFFRACTOMETER	40.0 m	9	
1		BEAMLINE 06 TD	SANS INSTRUMENT	14.0 m	8	SUPER-CRITICAL H2
1		BEAMLINE 05 TD	10 - 100 MICROVOLT SPECTROMETER	43.0 m	7	NON-POISONED (20 K)
1		BEAMLINE 04 TD	4B LIQUIDS REFLECTOMETER	10.0 m	6	COUPLED
1		BEAMLINE 04 TD	4A MAGNETISM REFLECTOMETER	12.0 m	5	
1		BEAMLINE 03 TU	TRIPLE AXIS SPECTROMETER	40.0 m	4	SUPER-CRITICAL H2
1		BEAMLINE 02 TU	CRYSTAL ANALYZER MICROVOLT SPECTROMETER	84.0 m	3	POISONED (20 K)
1		BEAMLINE 01 TU	1B SPECIAL PURPOSE SANS	30.9 m	2	DECOUPLED
1		BEAMLINE 01 TU	1A HIGH PRESSURE DIFFRACTOMETER	21.3 m	1	

NOTE: MODERATORS BU & BD MAY BE CHANGED TO POISONED, COMPOSITE, (H2/H2O)

NEXT ASSEMBLY

Figure 1

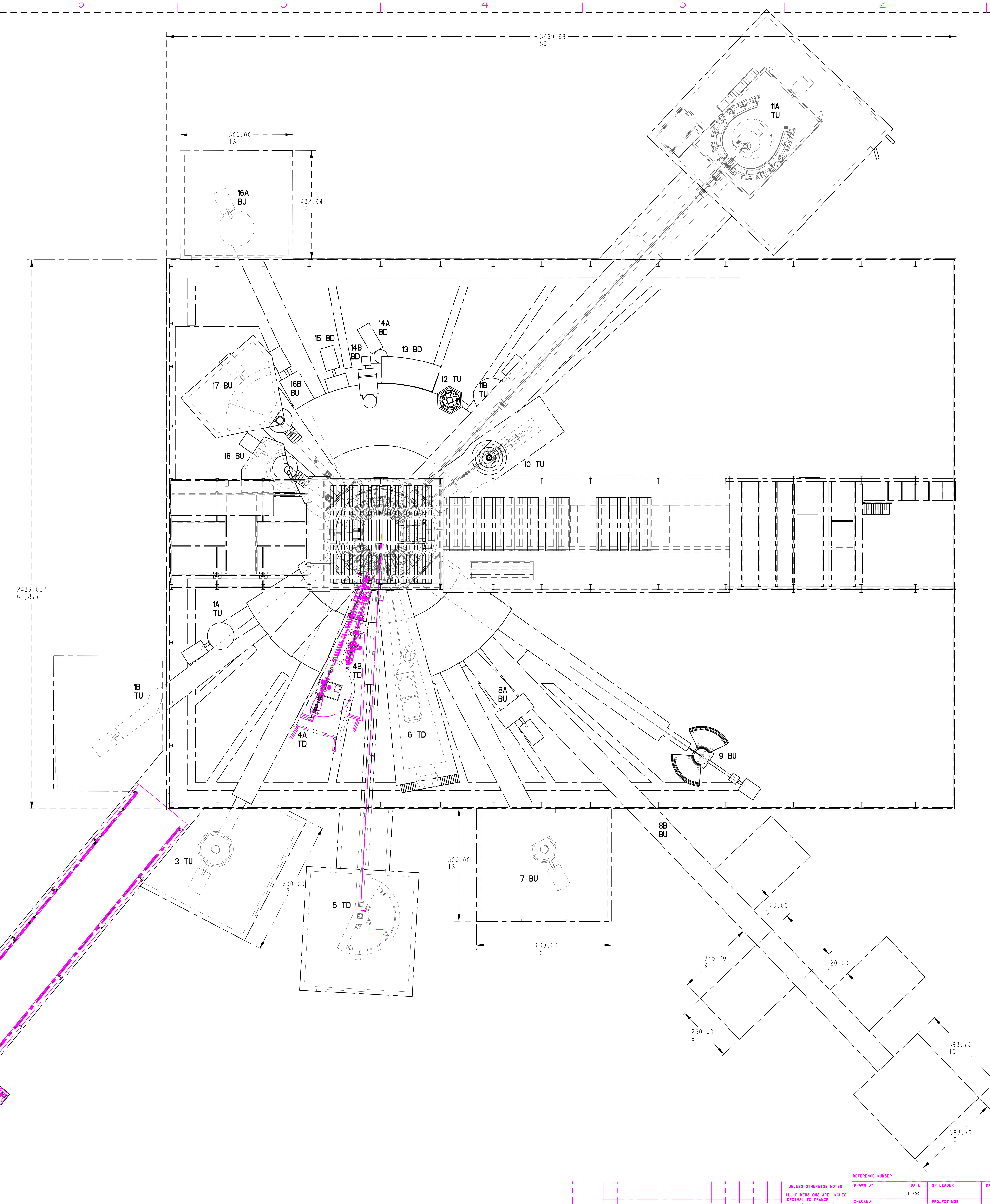

THIS DRAWING IS THE PROPERTY OF ARGONNE NATIONAL LABORATORY

Spallation Neutron Source

TITLE

Target Building

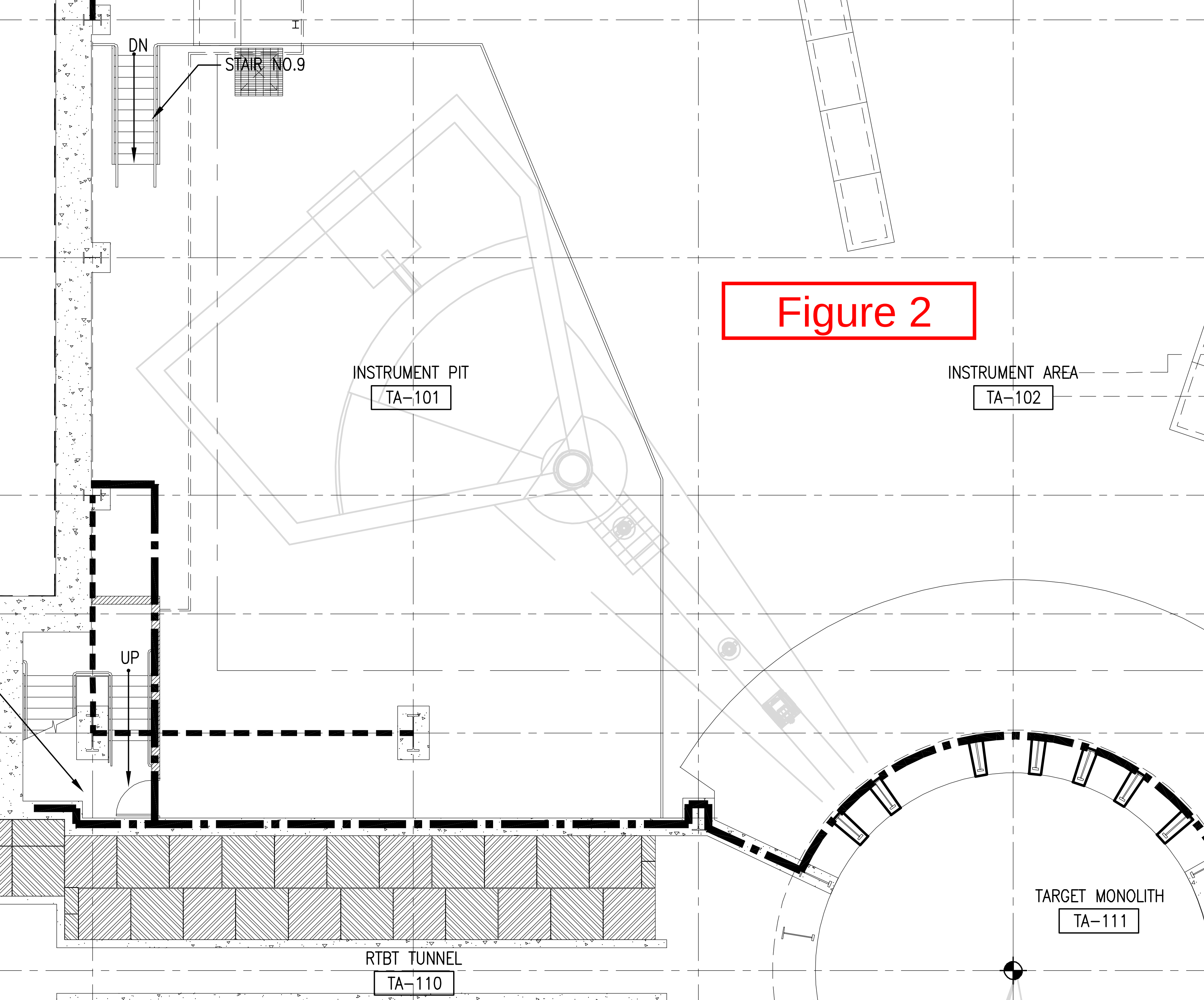
DN
STAIR NO.9
UP
INSTRUMENT PIT
TA-101
INSTRUMENT AREA
TA-102
TARGET MONOLITH
TA-111
RTBT TUNNEL
TA-110

Figure 2

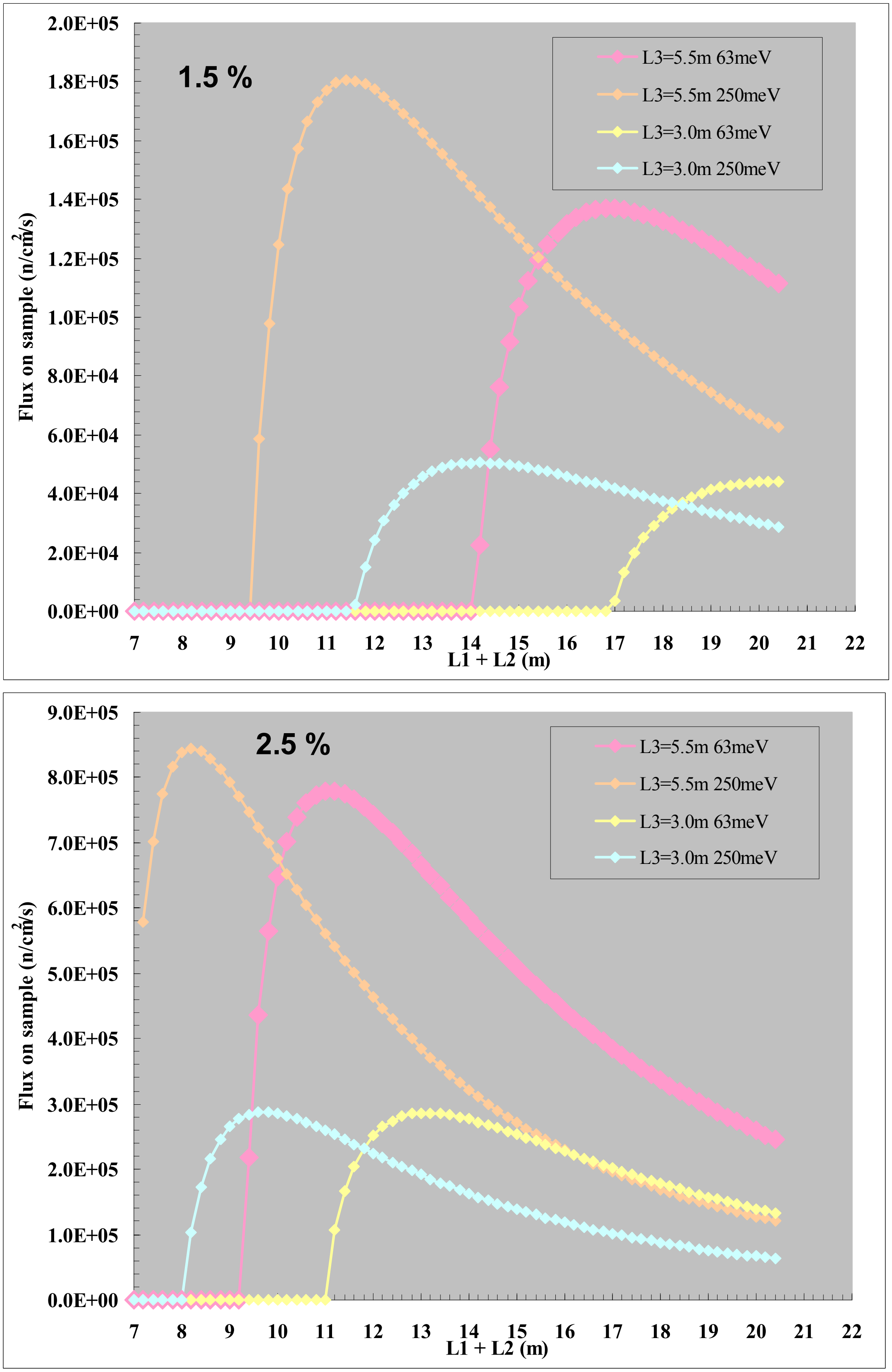

Figure 3. Flux on sample versus incident flightpath for 1.5% and 2.5% energy resolution

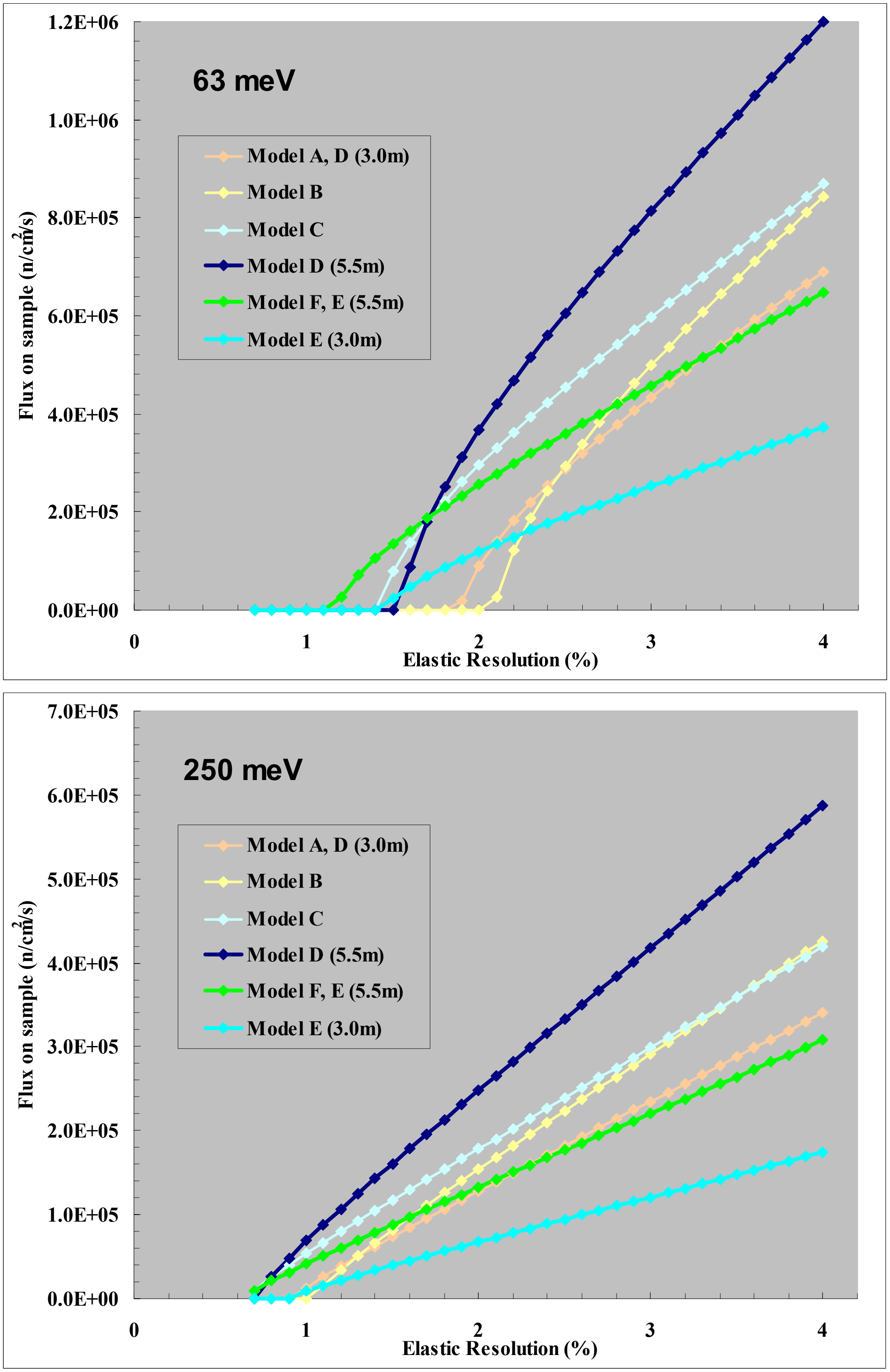

Figure 4. Flux on sample versus elastic resolution for the various detector banks.

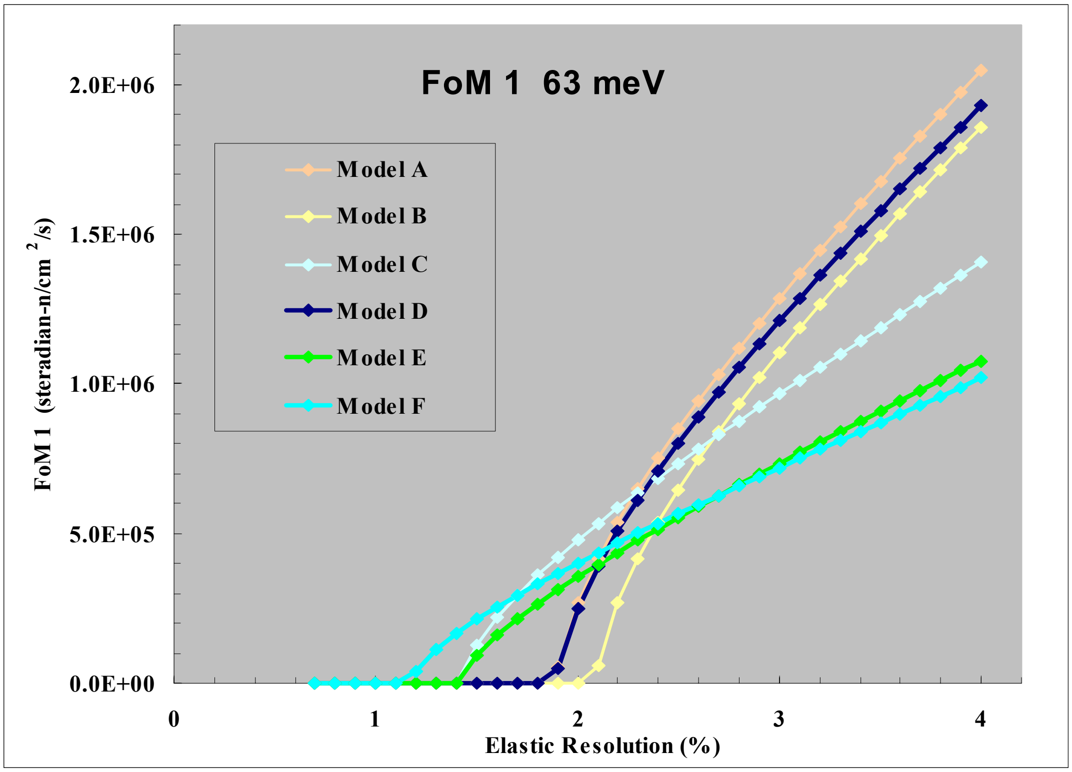

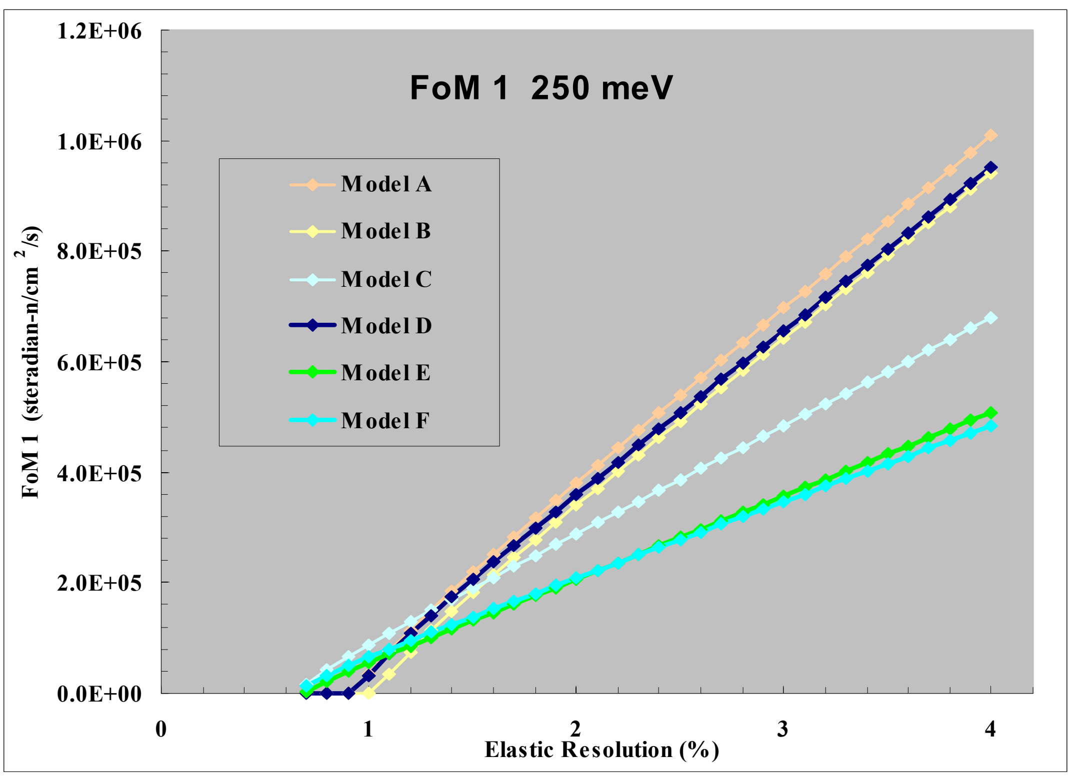

Figure 5. First figure-of-merit – flux on sample for lowest resolution bank times total solid angle.

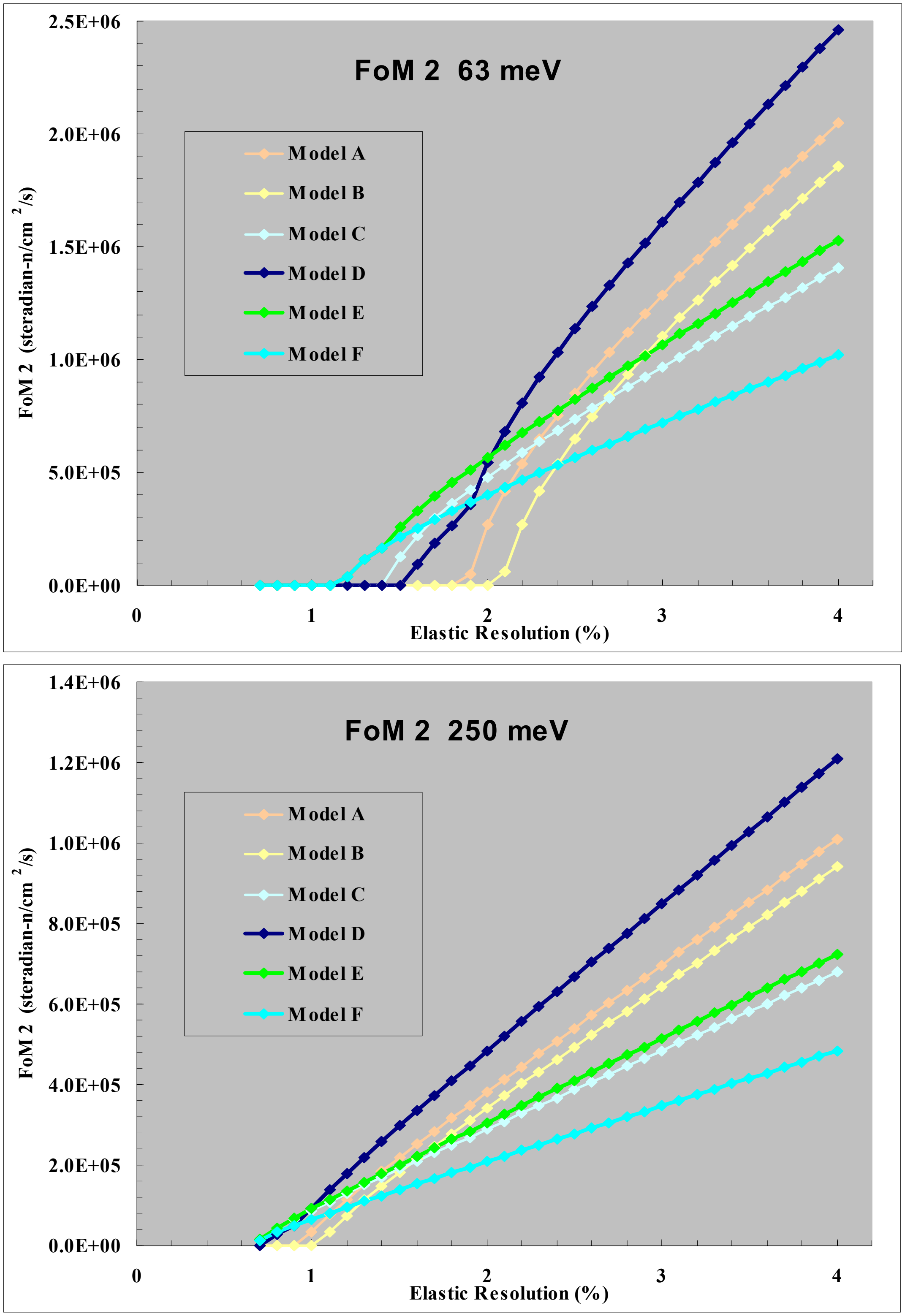

Figure 6. Second figure-of-merit – sum of flux on sample for each bank times each bank's solid angle.